BIOCHEMISTRY
including biophysical chemistry & molecular biology

Article

pubs.acs.org/biochemistry

The Role of Glu41 in the Binding of Dimannose to P51G-m4-CVN

Sai Kumar Ramadugu,[†] Zhen Li,[†] Hemant K. Kashyap, and Claudio J. Margulis*

Department of Chemistry, University of Iowa, 118 IATL, Iowa City, Iowa 52241, United States

Supporting Information

ABSTRACT: The carbohydrate binding protein, Cyanovirin-N, obtained from cyanobacteria, consists of high-affinity and low-affinity binding domains. To avoid the formation of a domain swapped structure in solution and also to better focus on the binding of carbohydrates at the high-affinity site, the Ghirlanda group (*Biochemistry*, *46*, 2007, 9199−9207) engineered the P51G-m4-CVN mutant which does not dimerize nor binds at the low-affinity site. This mutant provides an excellent starting point for the experimental and computational study of further transformations to enhance binding at the high-affinity site as well as to retool this site for the possible binding of different sugars. However, before such endeavors are pursued, detailed understanding of apparently key interactions both present in wild-type and P51G-m4-CVN at the high-affinity site must be derived and controversies about the importance of certain residues must be resolved. One such interaction is that of Glu41, a charged residue in intimate contact with 2′OH of dimannose at the nonreducing end. We do so computationally by performing two mutations using the thermodynamic integration formalism in explicit solvent. Mutations of P51G-m4-CVN Glu41 to Ala41 and Gly41 reveal that whereas the loss of Coulomb interactions result in a free energy penalty of about 2.1 kcal/mol, this is significantly compensated by favorable contributions to the Lennard-Jones portion of the transformation, resulting in almost no change in the free energy of binding. At least in terms of free energetics, and in the case of this particular CVN mutant, Glu41 does not appear to be as important as previously thought. This is not because of lack of extensive hydrogen bonding with the ligand but instead because of other compensating factors.

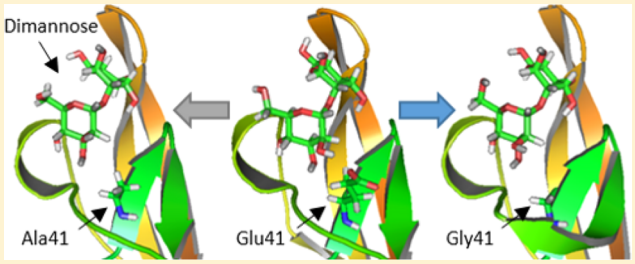

Cyanovirin-N (CVN) is a lectin of blue−green algae commonly called cyanobacteria (*Nostoc ellipsosporum*).[1] It binds Manα1−2Man motifs present in moderately complex carbohydrates such as high mannose which decorate the surface of gp120 present on HIV and SIV. The first published structure of wild-type CVN was obtained using NMR spectroscopy and was determined to be in the monomeric form.[2] CVN has two domains that are pseudosymmetric. Domain A spans residues 1−38 and 90−101, while residues 39−89 form domain B.[2] More than 10 different NMR or X-ray published structures of CVN and its mutants exist, some of them in the monomeric state and some others in a domain-swapped dimeric state.[3−13] A significant number of important computational studies addressing different aspects of these systems have also been published.[14−18] It is believed[13,19] that conversion of monomer to domain-swapped dimer occurs due to strain caused by the proline residue at 51 position (P51). Recent computational findings support this idea.[18]

Interestingly, whereas the mutation P51G stabilizes the monomeric state as well as a set of different possible oligomeric states,[20] the mutation S52P also in the hinge region appears to render it exclusively in domain-swapped dimeric form.[21] Each of the two domains in CVN can bind Manα1−2Man, which is the terminal part of the high mannose oligosaccharides (Man_9). Bewley et al. have shown that dimannose binds to domain B with high affinity and to domain A with low affinity.[22] In a later article, Bewley et al. mapped the binding site residues that appear to contribute the most to the binding at the high-affinity site (domain B) and at the low-affinity site (domain A). At the high-affinity site, Bewley identifies Glu41, Ser52, Asn53, Glu56, Thr57, Lys74, Thr75, Arg76, and Gln78 as key residues for binding. These residues interact either via hydrogen bonds and/or electrostatic interactions.[23] Key residues in the low-affinity site are identified as Lys3, Gln6, Thr7, Glu23, and Thr25.[23]

Molecular dynamics (MD) simulations of dimannose bound to the low- and high-affinity sites of wild-type CVN by Margulis have shown that, at the high-affinity site, Glu41 and Arg76 appear to be important in terms of their electrostatic interactions with Manα1−2Man.[14] Margulis also predicted a gating or trapping mechanism in which Arg76 caps dimannose. The role of Arg76 in conformational gating was later confirmed by Fromme et al. in their X-ray crystal studies, as they found two distinct distributions of Arg76 in the close and open conformation with reference to dimannose at the binding pocket.[13] Important studies on the binding and discrimination of trisaccharides at the high- and low-affinity binding sites are also available for wild-type CVN.[24]

Fujimoto et al. have used MD simulations coupled with a molecular mechanics Poisson−Boltzmann surface area (MM/PBSA) approach to study the binding affinity of Manα1−2Man and Manα1−2Manα1−2Man at the high- and low-affinity

Received: October 16, 2013
Revised: February 7, 2014
Published: February 13, 2014

 © 2014 American Chemical Society dx.doi.org/10.1021/bi4014159 | *Biochemistry* 2014, 53, 1477−1484

binding sites of wild-type CVN. Using this MD/MM/PBSA approach, they computed the difference in binding affinities[15] at the two protein sites and found in accordance to experiment[22,24] that binding to the high-affinity was significantly more important than that at the low-affinity site.

Botos et al. have shown in their crystal structural studies[25] that oligomannoses, Man_9 and Man_6, bind to the low-affinity site of CVN as a domain-swapped dimer. Sandström et al. applied saturation transfer difference NMR spectroscopy in the solution phase to show that both high- and low-affinity sites of domain swapped dimer bind di- and trisaccharides. Saturation transfer was observed for H2, H3, and H4 of the nonreducing end of dimannose.[26] Similar observations were made by Shenoy et al. using a synthetic analogue of Man_9 and Man_8.[27]

To determine whether the high-affinity site or the low-affinity site are required for antiviral activity, Barrientos et al. engineered a new set of mutants, CVN^{mutDA}, CVN^{mutDB}, and P51G-CVN.[28] Their conclusions were that an intact high-affinity site (domain B) was required for significant binding but domain A was important for cross-linking oligosaccharides on the surface of viral glycoproteins. Later, it was demonstrated that the existence of any two binding domains, irrespective of their identities, was sufficient to retain antiviral activity.[12,29]

Fromme et al. engineered yet a new mutant, P51G-m4-CVN.[12] The purpose for this was to enforce the monomeric structure (P51G mutation) and to abolish the activity of the low-affinity site (m4). The four mutations at the low-affinity site in this case are K3N, T7A, E23I, and N93A. The structure of P51G-m4-CVN was solved using X-ray crystallography. As expected, the protein was found to be in the monomer form and binds dimannose only at the high-affinity site.[12] Vorontsov et al. carried out the first computational studies[16,17] on the P51G-m4-CVN mutant coupled to dimannose and a set of dideoxy mannose ligands. Their MM/PBSA study shows that 3′OH and 4′OH of dimannose establish hydrogen bonds with high-affinity site residues which are abolished in the case of the dideoxy dimannose analogues. This results in much lower affinity of the dideoxy dimannose analogues. In the first study, key residues at the high-affinity were identified as Asn42, Asp44, Ser52, Asn53, Thr57, Lys74, and Thr75,[16] and in the free energy calculation using MM/(GB)PBSA approach, Asn42 and Thr57 were highlighted as important for preserving the hydrogen bonding network.[17] Interestingly, Arg76, but more importantly Glu41, perceived as key to binding in experimental studies[12,13,23] and computational studies[14,15,18] on wild-type CVN, did not appear to be so in these studies.[16,17] The authors proposed[16] a possible force field dependence on this result, and we expand on this issue below. This apparent discrepancy in part motivates the current work.

METHODS

System Preparation. The coordinates of the P51G-m4-CVN protein developed in the Ghirlanda lab[13] (PDB ID 2RDK) bound to Manα1−2Man were downloaded from the Protein Data Bank site www.pdb.org. In the present study, two mutants of P51G-m4-CVN, namely E41A-P51G-m4-CVN and E41G-P51G-m4-CVN, were generated by deleting the additional atoms in the Glu41 residue and renaming this residue to Ala41 or Gly41. P51G-m4-CVN, E41A-P51G-m4-CVN, and E41G-P51G-m4-CVN in complex with dimannose were solvated in a TIP3P[30] water box containing 15103 solvent molecules, resulting in a cubic box of dimensions 78 × 78 × 78 Å^3. The OPLS-AA force field for proteins[31,32] combined with the OPLS force field for carbohydrates[33] was used to simulate the protein−sugar complexes using Gromacs version 4.5.x.[34] Because the OPLS-AA for carbohydrates provides parameters only for hexopyranoses, small modifications to the partial charges in the glycosidic bond region were necessary to yield the disaccharide neutral. All dimannose force field parameters are provided as Supporting Information. P51G-m4-CVN has a charge of −3 electron units. Therefore 3 K^+ ions were added to maintain electroneutrality of the system. For the mutants E41A-P51G-m4-CVN and E41G-P51G-m4-CVN 3 K^+ were also added to keep the number of counterions the same across our thermodynamic cycle.

Initially, all the protein−sugar complexes were energy minimized using a steepest-descent protocol for 5000 steps. After the initial 3000 steps, the potential energy remained nearly constant for the rest of the minimization steps. Following minimization, 100 ps were run in the NVT (constant number of particles, N, volume, V, and temperature, T = 300K) ensemble followed by at least 5 ns of further equilibration in the NPT ensemble (constant number of particles, N, pressure, P = 1 bar, and temperature, T = 300K).

All subsequent simulations were also carried out at 300K and used the particle-mesh Ewald (PME)[35] protocol with a real space cutoff of 10 Å, grid size of 1 Å, and PME order of 6 to properly describe the electrostatic interactions. From the last 1 ns of the NPT equilibration, three snapshots separated by at least 250 ps were saved for running free energy calculations.

Simulations in the absence of dimannose use the same force field parameters, simulation protocols, and include the same number of water molecules and counterions.

Whereas all our free energy calculations are carried out using the OPLS-AA force field, in order to address issues related to the force dependence of certain results, we have also run some simulations using the Amber ff99SB[36] force field coupled with Glycam06[37] as implemented in the Amber code.[38]

Free Energy Simulations. The objective of our free energy calculations is to computationally estimate the difference in binding free energy between dimannose bound to P51G-m4-CVN and dimannose bound to each of the two mutants.

We sought the quantity $\Delta G_3 - \Delta G_4$ in Figure 1 which is equal to $\Delta G_1 - \Delta G_2$. Whereas thermodynamically either one of these two free energy subtractions is equivalent, $\Delta G_1 - \Delta G_2$ is

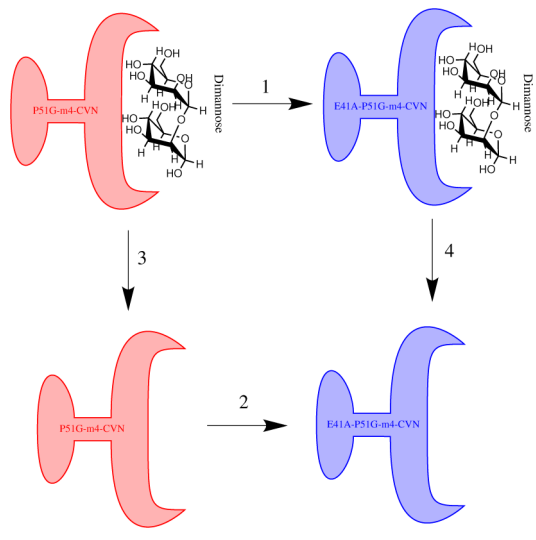

Figure 1. Thermodynamic cycle to compute the binding free energy difference for the mutation E41A(G).

dx.doi.org/10.1021/bi4014159 | Biochemistry 2014, 53, 1477−1484

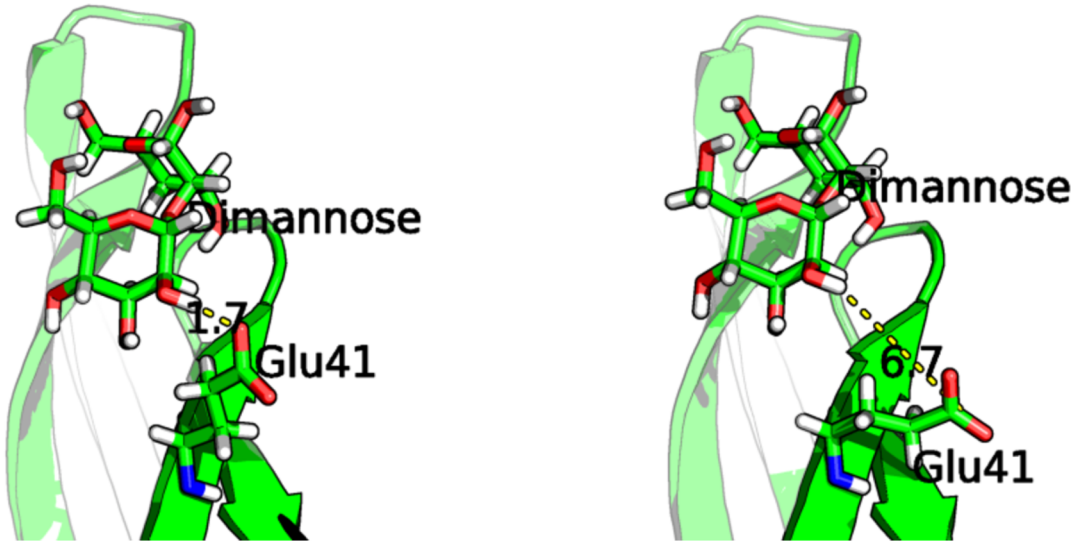

(a) Trans Configuration (b) Gauche Configuration

Figure 2. (a) χ1 of Glu 41 is in the trans conformation centered around 180° and the side chain of Glu41 is able to establish strong hydrogen bonding with 2′OH of the nonreducing end of dimannose. (b) χ1 of Glu41 is in the gauche conformation centered around 60° and its side chain is unable to establish hydrogen bonds with 2′OH of the nonreducing end of dimannose. In both figures, the protein backbone is represented with a large green arrow.

computationally more tractable because it does not involve the removal of the ligand. $\Delta G_1 - \Delta G_2$ requires the alchemical mutation of E41 to A41 or G41 in the presence (ΔG_1) and in the absence (ΔG_2) of dimannose.

In this study, ΔG_1 and ΔG_2 were further split into three processes, namely the Coulombic discharging of E41, the transformation of the Lennard-Jones interactions of E41 into those of A41 or G41, and the charging of A41 or G41. In our calculations, we computed the free energy of charging of A41 and G41 as the negative of the free energy of discharging.

In the present study, we utilized the single topology approach[39] in which simulations with $\lambda = 0$ utilize the force field parameters of the glutamate side chain and in which simulations with $\lambda = 1$ utilize the force field parameters of alanine or glycine. The extra atoms from glutamate are converted into dummy atoms as a series of simulations transform λ from 0 to 1. For the Lennard-Jones (LJ) portion of the transformation, we employed the soft-core potential approach[40,41] as coded in Gromacs with parameters $\alpha = 0.5$, $n = 1$, and $m = 1$, which have been previously shown to produce less error[42] and which are default values in Gromacs version 4.5.x.

Because in the case of the Coulombic discharge $\langle \partial V/\partial \lambda \rangle$, the quantity to be integrated to obtain free energy changes is fairly smooth, we used only 11 equally spaced λ values from 0 to 1. Instead, to reduce integration noise, for the Lennard-Jones transformation, we split the calculation into three parts. In the λ interval from 0 to 0.1 and 0.9 to 1, we ran calculations with λ increments of 0.02. Instead, we used 0.1 increments in the intermediate region between $\lambda = 0.1$ and $\lambda = 0.9$.

For each λ production run the protocol was as follows; first we performed a minimization of 5000 steps followed by equilibration of 100 ps in the NVT ensemble, then we further equilibrated in the NPT ensemble for another 200 ps to finally generate a production run of 2 ns in the NPT ensemble.

Three repetitions with different initial conditions of the three-step approach in the presence and absence of dimannose resulted in a total of 0.85 μs of combined simulation for the E41A and E41G mutations.

For the analysis of our free energy data and the estimation of errors, we utilized the g_bar program in which the Bennett Acceptance Ratio (BAR) method was implemented[43] as coded in Gromacs 4.5.x. This provides independent estimations of the error for each of the three steps of each of the three independent trials. However, we find that in some cases these errors were smaller than the differences in average free energy values across trials. Therefore, having three trials was very important to accurately represent our results.

RESULTS AND DISCUSSION

In prior NMR studies, Bewley and co-workers found that Glu41 appeared to strongly hydrogen bond to 2′OH of dimannose.[23] This is also the case in the analysis of the P51G-m4-CVN mutant structure obtained by Fromme et al.[13]

Careful scrutiny of all published monomeric and domain-swapped dimeric forms of CVN and its mutants shows that the χ1 dihedral angle of Glu41 has two populations. In monomeric structures of CVN, whether in presence or absence of dimannose, χ1 is reported to be in the trans configuration (with a value in the vicinity of 180°).[2,12,13,23] Interestingly, in almost all domain-swapped dimeric structures, χ1 is in the gauche configuration with angle range from 45° to 75°.[3,11,25,44]

This is not a minor detail because the trans configuration puts Glu41 in intimate contact with the sugar, whereas the gauche configuration puts the carboxylate part of the side chain away from the sugar unable to participate in hydrogen bonding (see Figure 2).

It turns out that, at least in the presence of dimannose, the Amber ff99SB[36] force field appears to favor the gauche conformation of χ1, instead the OPLS-AA force field appears instead to favor the trans conformation of χ1.

This force field difference plays an important role during molecular dynamics simulations. Figure 3 shows distances between oxygen atoms in the side chain of Glu41 and 2′ hydroxyl of the nonreducing end of dimannose as a function of time during MD simulation when using ff99SB coupled with the

dx.doi.org/10.1021/bi4014159 | Biochemistry 2014, 53, 1477−1484

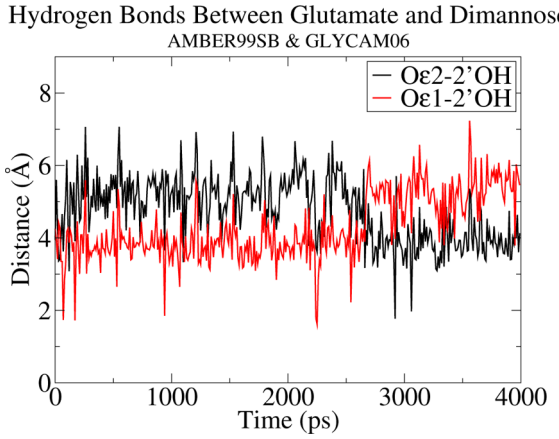

Figure 3. Hydrogen bond distance between carboxylate oxygens of side chain of glutamate and 2′OH of nonreducing end of dimannose using the AMBER11 software with the ff99SB force field for proteins and the GLYCAM06 force field for dimannose.

Glycam06 force field for sugars. It is clear that except in a few instances no oxygen comes in hydrogen bonding contact with 2′OH. This is in contrast to what one finds in a simulation based on the OPLS-AA force field where all the time there is hydrogen bonding contact. This can be seen in Figure 4. This supports the idea put forth by Vorontsov and co-workers about the force field dependence of this result.[16]

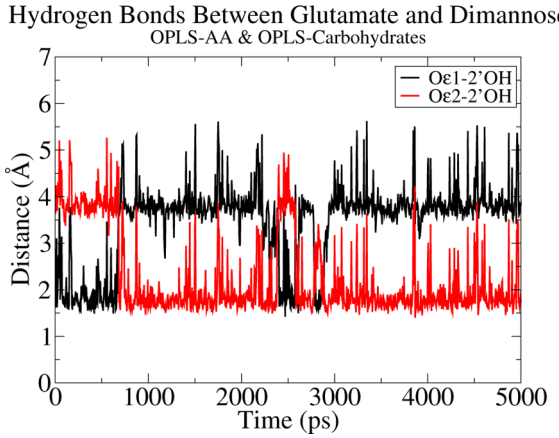

Figure 4. Hydrogen bond distance between carboxylate oxygens of side chain of glutamate and 2′OH of nonreducing end of dimannose using the Gromacs software suite coupled to the OPLS-AA force field for protein and the OPLS-Carbohydrates force field for dimannose.

Because in the monomeric form of CVN and its mutants $\chi 1$ of Glu41 have been shown experimentally to be almost exclusively in the trans conformation and because the results presented in Figures 3 and 4 indicate that of the two force fields probed only OPLS-AA[31,32] reproduced this important experimental result, we have chosen to use only this force field to perform a set of detailed thermodynamic cycles to unravel the difference in free energy of binding between dimannose in complex with P51G-m4-CVN as compared to E41A as well as E41G mutants.

We use the BAR approach in order to estimate the relative binding free energy difference of dimannose when P51G-m4-CVN is mutated at position 41 to Ala or Gly. Whereas these numbers can be experimentally obtained, our goal is to also develop important intuition regarding the relevance of structurally derived information such as hydrogen bonding to the ligand in the bound state. Furthermore, this approach will allow us to dissect free energetic information into different interaction components such as charge and dispersion forces. The relevance of this type of analysis has been highlighted repeatedly since the early work by Karplus and collaborators.[45]

We performed three trials for this mutational analysis as stated in the Methods section, and as shown in Figure 1, each trial has three steps, each of the steps in the presence of dimannose and absence of dimannose. Further, each step has λ ranging from 0 to 1. For the E41A mutation, we have 82 simulations for each trial and each λ simulation runs for 2 ns, resulting in 492 ns for all the trials. Because the Coulombic discharge of Glu41 is a common step in the thermodynamic cycle of both studied mutations, for the E41G mutation, we only needed 60 extra simulations for each trial, resulting in a total of 360 ns. Tables 1 and 2 summarize the results obtained for each step in the presence and absence of dimannose for both mutations.

One could predict, and this is indeed the case from simulation results shown in Tables 1 and 2, that a very large free energetic penalty is incurred upon Coulombic discharging of Glu41, a surface charged residue in intimate contact with dimannose. This penalty, which is on the order of 177 kcal/mol, is the result of interactions lost with the sugar and the environment. The reader is cautioned against directly comparing the absolute discharging free energy in the case of Ala41 or Gly41 against that of Glu41 while using PME. Because the overall charge (protein plus ions) of our system is different in the case of P51G-m4-CVN and the two mutants, such direct comparison is problematic. There is no problem, however, when using a thermodynamic cycle because the same overall charge exists in each case for simulations in the presence and absence of ligand. With this caveat in mind, it is still clear that the discharge of Ala or Gly in the presence of dimannose results in a penalty that is much smaller than required to discharge Glu. It is therefore quite reasonable to expect NMR and X-ray experiments as well as simulations to display strong hydrogen bonding between Glu41 and the 2OH′ of dimannose nonreducing end. However, what is often missed in the type of qualitative analysis that focuses only on interactions in the ligand-bound state is that the relative binding free energy is not only indicative of the strength of interactions in the ligand-bound state but also of the free energetics of the ligand-free transformation. What we mean by this is that whereas the charge transformation portion of ΔG_1 (the free energy of discharging Glu41 in the presence of dimannose) is a large positive number so is the discharging portion of ΔG_2 (the same process but in the absence of ligand). The discharging of Glu41 is very disfavorable as this is a surface charged residue exposed either to the ligand or in the absence of ligand to the solvent. Whereas Coulomb interactions between Glu41 and 2OH′ can indeed be very strong in the bound state,[14] so are the interactions of Glu41 and its solvent environment in the absence of ligand, and this is the cause of large cancellations when computing $\Delta\Delta G$.

It is therefore very important that experimental hydrogen bonding contacts between dimannose and the binding site be considered relevant for free energetics only after careful scrutiny of the same type of interactions in the absence of ligand.

Our study predicts that the difference in free energy penalties for the discharge Glu41 in the presence and absence of dimannose is on the order of 2.1 kcal/mol. To be more specific, whereas it costs about 177 kcal/mol to discharge Glu41 in the presence of the sugar, it only costs about 175 kcal/mol to do this in the absence of ligand (see Table 1 and Figures 5a and 6a).

dx.doi.org/10.1021/bi4014159 | *Biochemistry* 2014, 53, 1477−1484

Table 1. BAR Analysis for Relative Binding Free Energies for the Glu41Ala Mutation[a]

	discharging of Glu41 (kcal/mol)	LJ transformation (kcal/mol)	negative of discharging of Ala41 (kcal/mol)	total ΔG (kcal/mol)
trial I + dimannose	177.15 (0.18)	−2.35 (0.17)	−65.77 (0.03)	
trial II + dimannose	177.60 (0.17)	−2.83 (0.19)	−65.71 (0.05)	
trial III + dimannose	177.28 (0.08)	−2.72 (0.10)	−65.70 (0.03)	
AVG ΔG dimannose	177.34 [0.23]	−2.64 [0.25]	−65.73 [0.04]	108.98 [0.34]
trial I − dimannose	175.24 (0.17)	−1.14 (0.08)	−65.23 (0.06)	
trial II − dimannose	175.22 (0.16)	−0.98 (0.15)	−65.38 (0.08)	
trial III − dimannose	175.22 (0.27)	−0.81 (0.11)	−65.24 (0.06)	
AVG ΔG no dimannose	175.23 [0.21]	−0.98 [0.17]	−65.29 [0.08]	108.96 [0.28]
$\Delta\Delta G$	2.12 [0.31]	−1.66 [0.30]	−0.44 [0.09]	0.02 [0.44]

[a]The error values in the parentheses are those obtained from the g_bar utility available in the Gromacs package version 4.5.x which uses the Bennett Acceptance Ratio Method[43] to obtain the free energies. The errors reported for the average ΔG are either derived from the g_bar analysis or the standard deviation of the three trials, whichever is larger.

Table 2. BAR Analysis for Relative Binding Free Energies for the Glu41Gly Mutation[a]

	discharging of Glu41 (kcal/mol)	LJ transformation (kcal/mol)	negative of discharging of Gly41 (kcal/mol)	total ΔG (kcal/mol)
trial I + dimannose	177.15 (0.18)	−12.90 (0.13)	−64.97 (0.04)	
trial II + dimannose	177.60 (0.17)	−12.91 (0.27)	−65.03 (0.04)	
trial III + dimannose	177.28 (0.08)	−13.24 (0.15)	−64.93 (0.07)	
AVGΔG	177.34 [0.23]	−13.02 [0.22]	−64.98 [0.05]	99.35 [0.32]
trial I − dimannose	175.24 (0.17)	−10.98 (0.29)	−64.33 (0.03)	
trial II − dimannose	175.22 (0.16)	−10.88 (0.21)	−64.24 (0.01)	
trial III − dimannose	175.22 (0.27)	−10.83 (0.31)	−64.32 (0.02)	
AVGΔG	175.23 [0.21]	−10.90 [0.27]	−64.29 [0.05]	100.04 [0.35]
$\Delta\Delta G$	2.12 [0.31]	−2.12 [0.35]	−0.68 [0.07]	−0.69 [0.47]

[a]The values in the parentheses are the associated errors obtained from g_bar program in Gromacs version 4.5.x which uses the Bennett Acceptance Ratio Method[43] to obtain the free energies. The errors reported for the average ΔG are either the error obtained from the g_bar analysis or the standard deviation of the three trials, whichever is the larger value.

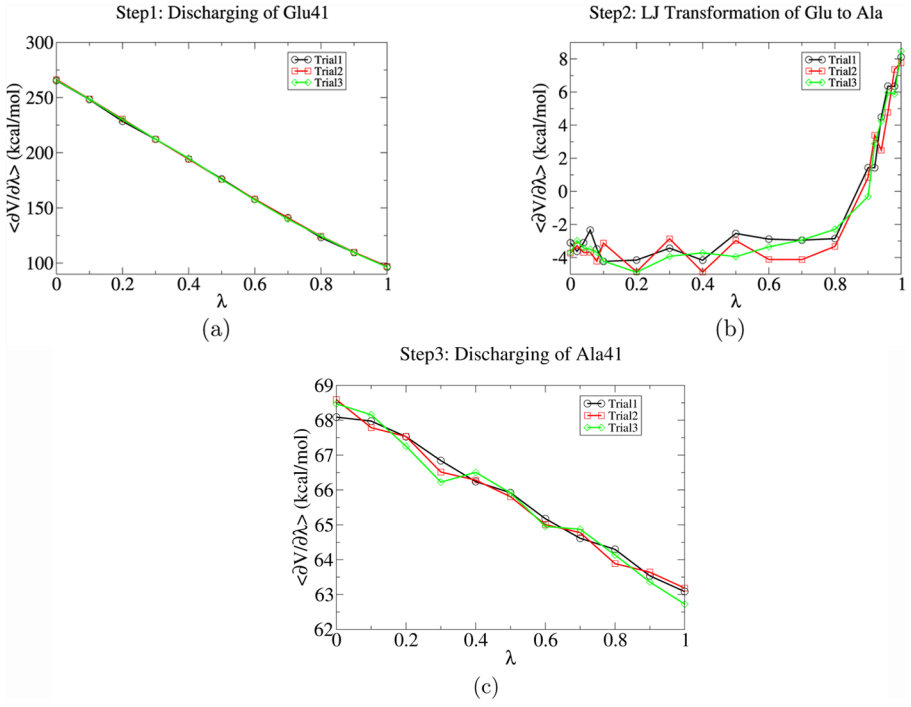

Figure 5. Three-step approach for thermodynamic integration simulations for Glu41Ala in presence of dimannose, trial I (black, circles), trial II (red squares), and trial III (green diamonds). Discharging of Glu (a), LJ transformation (b), discharging of Ala (c).

Furthermore, the overall Coulomb portion of $(\Delta G_1 - \Delta G_2)$ is on the order of 1.7 kcal/mol in the case of the E41A mutation and 1.4 kcal/mol in the case of the E41G mutation (see Tables 1 and 2). This is because the difference in discharging free energies for Ala41 or Gly41 in the presence and in the absence of sugar are on the order of 0.4 and 0.7 kcal/mol, respectively. Because the Coulombic $\Delta\Delta G$ for the discharge of Glu41 in the presence and absence of dimannose is significantly larger than the same free

dx.doi.org/10.1021/bi4014159 | *Biochemistry* 2014, 53, 1477−1484

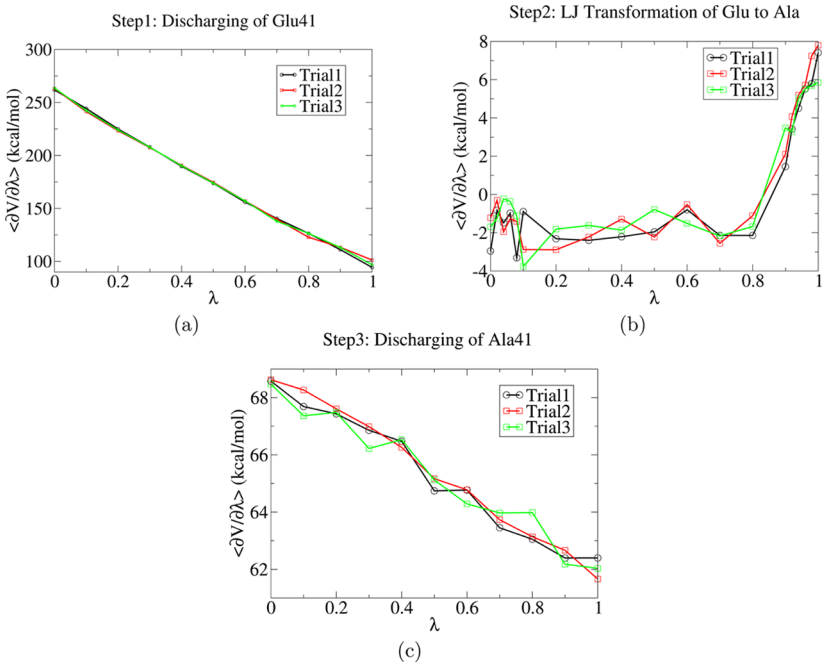

Figure 6. Three-step approach for thermodynamic integration simulations for Glu41Ala in absence of dimannose, trial I (black, circles), trial II (red squares), and trial III (green diamonds). Discharging of Glu (a), LJ transformation (b), discharging of Ala (c).

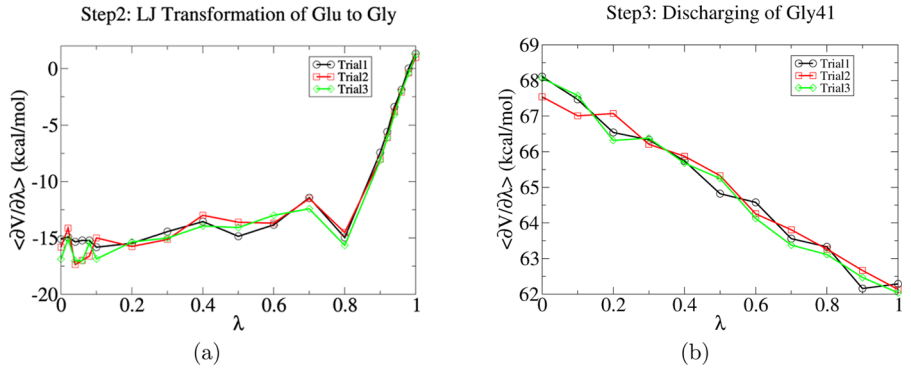

Figure 7. Three-step approach for thermodynamic integration simulations for Glu41Gly in the presence of dimannose, trial I (black, circles), trial II (red squares), and trial III (green diamonds). LJ transformation (a), discharging of Gly (b).

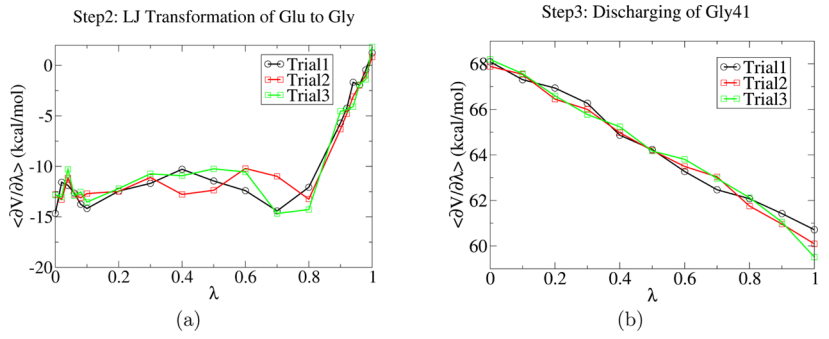

Figure 8. Three-step approach for thermodynamic integration simulations for Glu41Gly in the absence of dimannose, trial I (black, circles), trial II (red squares), and trial III (green diamonds). LJ transformation (a), discharging of Gly (b).

energy difference in the case of Ala and Gly, we conclude that Glu41 stabilizes the ligand from a Coulomb perspective.

What one learns from this portion of the analysis is that in the case of the mutation of the charged surface amino acid Glu41 to Ala41 or to Gly41, the Coulombic portion of the relative free energy of binding arises mostly due to the extra stabilization of Glu41 in the presence of the disaccharide as compared to Glu41 in the presence of solvent at the binding site. This is demonstrated in Figures 5a,c, 6a,c, 7b, and 8b as well as in Tables 1 and 2. If 1.7 kcal/mol was the binding free energy difference between the protein and dimannose when Glu41 is mutated to Ala or Gly, this would be quite significant. However

dx.doi.org/10.1021/bi4014159 | *Biochemistry* 2014, 53, 1477−1484

further cancellations occur due to dispersion interactions stabilization. A Gly side chain is smaller than an Ala side chain which in turn is smaller than a Glu side chain. In the particular case of binding to dimannose, the mutation of Glu41 into smaller residues appears to be free energetically favorable with respect to dispersion interactions. We find that from a dispersion interactions perspective, Gly is better than Ala which in turns is better than Glu. This can be appreciated from Figures 5b, 6b, 7a, and 8a and Tables 1 and 2. In the case of the E41A mutation, the dispersion contributions significantly diminish the energetic cost of the mutation and make the mutation E41G slightly favorable. This result could be seen as somewhat unexpected based purely on structural experimental conjectures or in light of our own previous molecular dynamics simulations showing very large electrostatic interaction between Glu41 in wild-type and the disaccharide but it is not. This is because for the interpretation of free energetics one should also consider the interactions with solvent in the ligand-free state.

■ CONCLUSIONS

This article describes a detailed analysis of the importance of Glu41 to the relative binding free energy of dimannose to P51G-m4-CVN and two mutants at position 41. Several interesting findings arise from this work. First, from a purely technical perspective, there appears to be some force field dependence on the most likely conformation of the $\chi 1$ angle of the side chain of Glu41 which impacts whether this residue is in close proximity of 2OH′ of the nonreducing end of dimannose. Experimental evidence appears to indicate that at least in the monomeric form $\chi 1$ should be in most cases in the trans conformation. Second, we find that although it is true that Glu41 strongly hydrogen bonds to 2OH′ of the nonreducing end of dimannose, this does not necessarily result in a very large relative free energy of binding penalty for the mutation of Glu41 into Ala41 or Gly41. Coulomb interactions of Glu41 in the presence of dimannose are very strong, but so are they with the environment in the absence of ligand. Replacing the Coulombic interactions between dimannose and a charged Glu41 costs on the order of 1.7 kcal/mol in the case of E41A and 1.4 kcal/mol in the case of E41G. However, these numbers are greatly diminished by favorable dispersion free energy changes. Briefly, the cost of losing hydrogen bond interactions between the ligand and Glu41 is compensated by better dispersion interactions with Ala or Gly.

In more general terms, we learn that it is perhaps unwise to assume that what appears to be a strong hydrogen bond during molecular dynamics simulations, NMR experiments, or X-ray crystallography will necessarily translate into a high importance interaction for relative free energetics of binding.

■ ASSOCIATED CONTENT

Supporting Information

Dihedral conformational details for dimannose in solution as well as bound to P51G-m4-CVN and its mutants; force field parameters for dimannose. This material is available free of charge via the Internet at http://pubs.acs.org.

■ AUTHOR INFORMATION

Corresponding Author

*Phone: 319-335-0615. E-mail: claudio-margulis@uiowa.edu.

Author Contributions

†S.K.R. and Z.L. contributed equally to this article

Funding

This work was funded by grant number MCB-1121134 from the National Science Foundation awarded to C.J.M.

Notes

The authors declare no competing financial interest.

■ ACKNOWLEDGMENTS

We thank Prof. George Kaminski, Prof. Harry Stern, Prof. Giovanna Ghirlanda, Prof. Banu Ozkan, and Prof. Francesca Massi for helpful discussions.

■ REFERENCES

(1) Boyd, M. R., Gustafson, K. R., McMahon, J. B., Shoemaker, R. H., O'Keefe, B. R., Mori, T., Gulakowski, R. J., Wu, L., Rivera, M. I., Laurencot, C. M., Currens, M. J., Cardellina, J. H., II, Buckheit, R. W., Jr., Nara, P. L., Pannell, L. K., Sowder, R. C., II, and Henderson, L. E. (1997) Discovery of cyanovirin-N, a novel human immunodeficiency virus-inactivating protein that binds viral surface envelope glycoprotein gp120: potential applications to microbicide development. *Antimicrob. Agents Chemother. 41*, 1521−1530.

(2) Bewley, C. A., Gustafson, K. R., Boyd, M. R., Covell, D. G., Bax, A., Clore, G. M., and Gronenborn, A. M. (1998) Solution structure of cyanovirin-N, a potent HIV-inactivating protein. *Nature Struct. Biol. 5*, 571−578.

(3) Barrientos, L. G., Louis, J. M., Botos, I., Mori, T., Han, Z., O'Keefe, B. R., Boyd, M. R., Wlodawer, A., and Gronenborn, A. M. (2002) The Domain-Swapped Dimer of Cyanovirin-N Is in a Metastable Folded State: Reconciliation of X-Ray and NMR Structures. *Structure 10*, 673−686.

(4) Bewley, C. A. (2001) Rapid Validation of the Overall Structure of an Internal Domain-Swapped Mutant of the Anti-HIV Protein Cyanovirin-N Using Residual Dipolar Couplings. *J. Am. Chem. Soc. 123*, 1014−1015.

(5) Bewley, C. A., and Clore, G. M. (2000) Determination of the Relative Orientation of the Two Halves of the Domain-Swapped Dimer of Cyanovirin-N in Solution Using Dipolar Couplings and Rigid Body Minimization. *J. Am. Chem. Soc. 122*, 6009−6016.

(6) Kelley, B. S., Chang, L. C., and Bewley, C. A. (2002) Engineering an Obligate Domain-Swapped Dimer of Cyanovirin-N with Enhanced Anti-HIV Activity. *J. Am. Chem. Soc. 124*, 3210−3211.

(7) Liu, L., Byeon, I.-J. L., Bahar, I., and Gronenborn, A. M. (2012) Domain Swapping Proceeds via Complete Unfolding: A ^{19}F- and ^{1}H-NMR Study of the Cyanovirin-N Protein. *J. Am. Chem. Soc. 134*, 4229−4235.

(8) Matei, E., Zheng, A., Furey, W., Rose, J., Aiken, C., and Gronenborn, A. M. (2010) Anti-HIV Activity of Defective Cyanovirin-N Mutants Is Restored by Dimerization. *J. Biol. Chem. 285*, 13057−13065.

(9) Yang, F., Bewley, C. A., Louis, J. M., Gustafson, K. R., Boyd, M. R., Gronenborn, A. M., Clore, G. M., and Wlodawer, A. (1999) Crystal structure of cyanovirin-N, a potent HIV-inactivating protein, shows unexpected domain swapping. *J. Mol. Biol. 288*, 403−412.

(10) Botos, I., and Wlodawer, A. (2003) Cyanovirin-N: a sugar-binding antiviral protein with a new twist. *Cell. Mol. Life Sci. 60*, 277−287.

(11) Botos, I., Mori, T., Cartner, L. K., Boyd, M. R., and Wlodawer, A. (2002) Domain-swapped structure of a mutant of cyanovirin-N. *Biochem. Biophys. Res. Commun. 294*, 184−190.

(12) Fromme, R., Katiliene, Z., Giomarelli, B., Bogani, F., Mc Mahon, J., Mori, T., Fromme, P., and Ghirlanda, G. (2007) A Monovalent Mutant of Cyanovirin-N Provides Insight into the Role of Multiple Interactions with gp120 for Antiviral Activity. *Biochemistry 46*, 9199−9207.

(13) Fromme, R., Katiliene, Z., Fromme, P., and Ghirlanda, G. (2008) Conformational gating of dimannose binding to the antiviral protein cyanovirin revealed from the crystal structure at 1.35 Å resolution. *Protein Sci. 17*, 939−944.

(14) Margulis, C. J. (2005) Computational Study of the Dynamics of Mannose Disaccharides Free in Solution and Bound to the Potent Anti-HIV Virucidal Protein Cyanovirin. *J. Phys. Chem. B 109*, 3639−3647.
(15) Fujimoto, Y. K., Terbush, R. N., Patsalo, V., and Green, D. F. (2008) Computational models explain the oligosaccharide specificity of cyanovirin-N. *Protein Sci. 17*, 2008−2014.
(16) Vorontsov, I. I., and Miyashita, O. (2009) Solution and crystal molecular dynamics simulation study of m4-cyanovirin-N mutants complexed with di-mannose. *Biophys. J. 97*, 2532−2540.
(17) Vorontsov, I. I., and Miyashita, O. (2011) Crystal molecular dynamics simulations to speed up MM/PB(GB)SA evaluation of binding free energies of di-mannose deoxy analogs with P51G-m4−Cyanovirin-N. *J. Comput. Chem. 32*, 1043−1053.
(18) Fujimoto, Y. K., and Green, D. F. (2012) Carbohydrate Recognition by the Antiviral Lectin Cyanovirin-N. *J. Am. Chem. Soc. 134*, 19639−19651.
(19) Barrientos, L. G., Lasala, F., Delgado, R., Sanchez, A., and Gronenborn, A. M. (2004) Flipping the Switch from Monomeric to Dimeric CV-N Has Little Effect on Antiviral Activity. *Structure 12*, 1799−1807.
(20) Koharudin, L. M., Liu, L., and Gronenborn, A. M. (2013) Different 3D domain-swapped oligomeric cyanovirin-N structures suggest trapped folding intermediates. *Proc. Natl. Acad. Sci. U. S. A. 110*, 7702−7707.
(21) Han, Z., Xiong, C., Mori, T., and Boyd, M. R. (2002) Discovery of a stable dimeric mutant of cyanovirin-N (CV-N) from a T7 phage-displayed CV-N mutant library. *Biochem. Biophys. Res. Commun. 292*, 1036−1043.
(22) Bewley, C. A., and Otero-Quintero, S. (2001) The Potent Anti-HIV Protein Cyanovirin-N Contains Two Novel Carbohydrate Binding Sites That Selectively Bind to Man8 D1D3 and Man9 with Nanomolar Affinity: Implications for Binding to the HIV Envelope Protein gp120. *J. Am. Chem. Soc. 123*, 3892−3902.
(23) Bewley, C. A. (2001) Solution Structure of a Cyanovirin-N:Manα1−2Manα Complex: Structural Basis for High-Affinity Carbohydrate-Mediated Binding to gp120. *Structure 9*, 931−940.
(24) Bewley, C. A., Kiyonaka, S., and Hamachi, I. (2002) Site-specific Discrimination by Cyanovirin-N for α-Linked Trisaccharides Comprising the Three Arms of Man8 and Man9. *J. Mol. Biol. 322*, 881−889.
(25) Botos, I., O'Keefe, B. R., Shenoy, S. R., Cartner, L. K., Ratner, D. M., Seeberger, P. H., Boyd, M. R., and Wlodawer, A. (2002) Structures of the Complexes of a Potent Anti-HIV Protein Cyanovirin-N and High Mannose Oligosaccharides. *J. Biol. Chem. 277*, 34336−34342.
(26) Sandström, C., Berteau, O., Gemma, E., Oscarson, S., Kenne, L., and Gronenborn, A. M. (2004) Atomic Mapping of the Interactions between the Antiviral Agent Cyanovirin-N and Oligomannosides by Saturation-Transfer Difference NMR. *Biochemistry 43*, 13926−13931.
(27) Shenoy, S. R., Barrientos, L. G., Ratner, D. M., O'Keefe, B. R., Seeberger, P. H., Gronenborn, A. M., and Boyd, M. R. (2002) Multisite and multivalent binding between cyanovirin-N and branched oligomannosides calorimetric and NMR characterization. *Chem. Biol. 9*, 1109−1118.
(28) Barrientos, L. G., Matei, E., Lasala, F., Delgado, R., and Gronenborn, A. M. (2006) Dissecting carbohydrate Cyanovirin-N binding by structure-guided mutagenesis: functional implications for viral entry inhibition. *Protein Eng., Des. Sel. 19*, 525−535.
(29) Liu, Y., Carroll, J. R., Holt, L. A., McMahon, J., Giomarelli, B., and Ghirlanda, G. (2009) Multivalent interactions with gp120 are required for the anti-HIV activity of Cyanovirin. *Peptide Sci. 92*, 194−200.
(30) Jorgensen, W. L., Chandrasekhar, J., Madura, J. D., Impey, R. W., and Klein, M. L. (1983) Comparison of simple potential functions for simulating liquid water. *J. Chem. Phys. 79*, 926−935.
(31) Jorgensen, W. L., Maxwell, D. S., and Tirado-Rives, J. (1996) Development and Testing of the OPLS All-Atom Force Field on Conformational Energetics and Properties of Organic Liquids. *J. Am. Chem. Soc. 118*, 11225−11236.
(32) Kaminski, G. A., Friesner, A. R., Tirado-Rives, J., and Jorgensen, W. L. (2001) Evaluation and Reparametrization of the OPLS-AA Force Field for Proteins via Comparison with Accurate Quantum Chemical Calculations on Peptides. *J. Phys. Chem. B 105*, 6474−6487.
(33) Damm, W., Frontera, A., Tirado-Rives, J., and Jorgensen, W. L. (1997) OPLS All-Atom Force Field for Carbohydrates. *J. Comput. Chem. 18*, 1955−1970.
(34) Hess, B., Kutzner, C., van der Spoel, D., and Lindhal, E. (2008) GROMACS 4: Algorithms for Highly Efficient, Load-Balanced, and Scalable Molecular Simulation. *J. Chem. Theory Comput. 4*, 435−447.
(35) Darden, T., York, D., and Pedersen, L. (1993) Particle mesh Ewald: An $N\log(N)$ method for Ewald sums in large systems. *J. Chem. Phys. 98*, 10089−10092.
(36) Hornak, V., Abel, R., Okur, A., Strockbine, B., Roitberg, A., and Simmerling, C. (2006) Comparison of multiple Amber force fields and development of improved protein backbone parameters. *Proteins: Struct., Funct., and Bioinform. 65*, 712−725.
(37) Kirschner, K. N., Yongye, A. B., Tschampel, J., Gonzalez-Outeirnino, S. M., Daniels, C. R., Foley, L. B., and Woods, R. J. (2008) GLYCAM06: A Generalizable Biomolecular Force Field. Carbohydrates. *J. Comput. Chem. 29*, 1−34.
(38) Case, D. A. et al. (2010) *Amber 11*, University of California, San Francisco.
(39) Pearlman, D. A. (1994) A Comparison of Alternative Approaches to Free Energy Calculations. *J. Phys. Chem. 98*, 1487−1493.
(40) Beutler, T. C., Mark, A. E., van Schaik, R. C., Gerber, P. R., and van Gunsteren, W. F. (2006) Avoiding singularities and numerical instabilities in free energy calculations based on molecular simulations. *Chem. Phys. Lett. 222*, 529−539.
(41) Steinbrecher, T., Mobley, D. L., and Case, D. A. (2007) Nonlinear scaling schemes for Lennard-Jones interactions in free energy calculations. *J. Chem. Phys. 127*, 214108−214120.
(42) Shirts, M. R., and Pande, V. S. (2005) Solvation free energies of amino acid side chains for common molecular mechanics water models. *J. Chem. Phys. 122*, 134508−134520.
(43) Bennett, C. H. (1976) Efficient estimation of free energy differences from Monte Carlo data. *J. Comput. Phys. 22*, 245−268.
(44) Clore, G. M., and Bewley, C. A. (2002) Using Conjoined Rigid Body/Torsion Angle Simulated Annealing to Determine the Relative Orientation of Covalently Linked Protein Domains from Dipolar Couplings. *J. Magn. Reson. 164*, 329−335.
(45) Boresch, S., and Karplus, M. (1995) The meaning of component analysis: decomposition of the free energy in terms of specific interactions. *J. Mol. Biol. 254*, 801−807.